

# White Light Velocimetry

David J. Erskine and Neil C. Holmes

erskinel@llnl.gov

*Lawrence Livermore National Laboratory, 5000 East Ave., Livermore CA 94551*

**Radiation reflected from a moving object experiences a Doppler shift in its frequency. This basic phenomenon underlies practical interferometric techniques for remote velocity measurement used widely in meteorology and law enforcement, as well as in medicine<sup>1</sup> (using acoustic waves) and other fields of science and engineering<sup>2-5</sup>. Existing velocimetric techniques use coherent quasi-monochromatic sources of illumination, which, for optical applications, generally limits practical sources to lasers operating in single-frequency mode. Such sources are not, however, sufficiently powerful for applications where simultaneous velocity measurements at many points on a target are desired. Here we describe a technique for remote velocity measurement that uses broadband incoherent illumination. The viability of this technique is demonstrated by measuring the velocity of a target moving at 16 m/s using white light from an incandescent source. Powerful, compact and inexpensive radiation sources (such as flash and arc lamps, or lasers operating at several wavelengths) can now be exploited for high-power applications of remote-target velocimetry.**

The VISAR<sup>2-5</sup> velocimeter (velocity interferometer system for any reflector) is an optical interferometer having a fixed delay  $\Delta$  between its arms. This delay converts small Doppler shifts into fringe shifts in the interferometer output. Let the delay be specified by the distance  $(c \Delta)$  light travels in that time, where  $c$  is the velocity of light in vacuum. The idealized velocity per fringe proportionality<sup>2,3</sup>  $(\Delta \lambda / \lambda)$  of a VISAR is

$$= \frac{c}{2(c \Delta)} \quad (1)$$

where  $\lambda$  is the average wavelength of light. For example, to measure highway velocities in green light with  $\Delta \lambda = 10$  m/s requires  $c \Delta = 8$  m. Equation (1) neglects dispersion<sup>3</sup> in the glass optics inside the interferometer and assumes  $v/c \ll 1$ .

In previous VISARs, the coherence length  $(\Delta \lambda)$  of the illumination must be as large as  $c \Delta$  in order to produce fringes with significant visibility. This severely restricted the kind of light source which could be used. The  $\Delta \lambda$  of white light ( $\sim 1.5 \mu\text{m}$ ) was insufficient. Previously, lasers were the only light sources used in VISARs because their

coherence length could be made sufficiently long when operated in a single frequency mode. However, in this mode the output power is low.

Because of this, typical laboratory measurements in shock physics were limited to measurement of velocity at a single point on the target. These experiments<sup>6-8</sup> can measure both the structure and arrival time of a shockwave after propagating through a sample-- information which can yield the equation of state (pressure versus volume), the transition between elastic and plastic flow (controlled by material strength), or the presence of phase transitions.

Such experiments can be greatly improved if we could measure sample velocity simultaneously at more than one point. For example, multi-point velocimetry on a wedged sample could show the evolution of the shockwave profile versus propagation depth. Moreover, measurements of velocity across a line or an area over a target could diagnose the chaotic motion of an accelerated and spatially perturbed interface between materials of unequal densities (called Rayleigh-Taylor<sup>9</sup> or Richtmeyer-Meshkov<sup>10</sup> instability, depending on details of the acceleration). This issue is relevant to implosions used in laser fusion.

Previously, multi-point or line<sup>11</sup> VISAR velocimetry has been very expensive. Lasers with sufficiently long coherence length were relatively weak, and required optical amplifiers to illuminate more than a single point. Velocimetry over a surface, or of a remote object through a telescope in the field demands orders of magnitude more power, particularly if multi-meter scale coherence lengths are needed (such as needed for resolving ~10 m/s velocities).

We have developed a simple and generic method (Fig. 1) of preparing any wave source, regardless of its initial coherence, to illuminate a velocity interferometric experiment. A coherent echo is imprinted on the illuminating light by an interferometer (denoted the source interferometer) having a delay  $\tau_s$ . The reflected light from the target is observed through a second interferometer (denoted the detecting interferometer) having delay  $\tau_d$ . Partial fringes result when  $\tau_s$  and  $\tau_d$  are within a coherence length of each other. Target velocity causes the apparent value of  $\tau_s$  to change due to the slight Doppler scaling of the spectrum reflected from the target, producing a fringe shift.

Double interferometer arrangements using short coherence length light have been used previously in communication<sup>12</sup> and to multiplex serial fiber optic sensors<sup>13</sup>, and to measure target motion where the target is internal to one of the interferometers<sup>14-16</sup>. However, we believe we are the first to apply this concept using ordinary lamps to remote targets external to an interferometer. [After publication, we learned of a laser illuminated double Fabry-Perot configuration by Gidon and Behar<sup>19</sup>]. This allows the fringe phase to

be independent of target distance, surface roughness, and the scattering and dispersive properties of the interposed medium. A single interferometer technique by Geindre et al.<sup>17</sup> measures high velocity (100 km/s) plasma by illuminating the plasma with two subpicosecond pulses separated by  $\sim 1$  ps, then dispersing the reflected light with a grating. Their Doppler shift is resolvable by a grating rather than a second interferometer because it is so large.

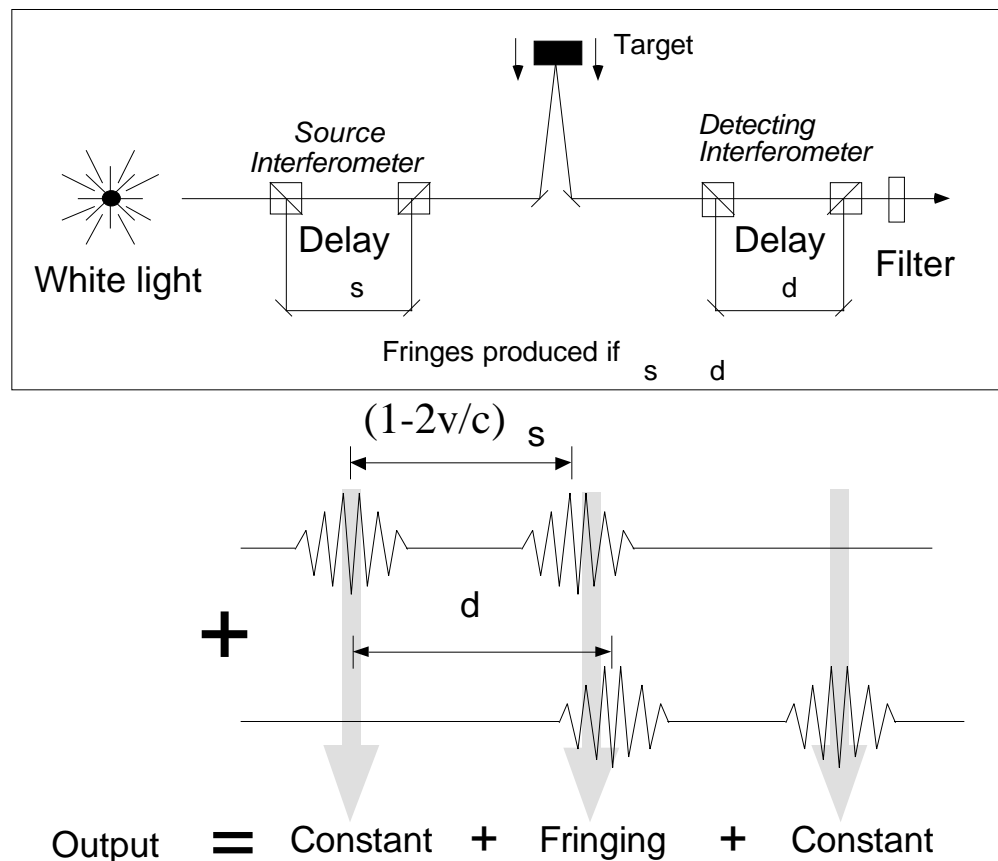


**Fig. 1.** White light velocimeter concept. Two interferometers before and after target have similar delays  $s$  and  $d$ . White light is a series of independent wave packets. The first interferometer splits each wave packet into two identical packets-- the second does the same to create a total of four. Two of those packets will overlap if  $s = d$ , producing fringes. The other packets contribute constant intensity. Target velocity will change the apparent  $s$  due to the Doppler effect, causing a fringe shift. The wave packet length is inversely proportional to system bandwidth, represented by the filter.

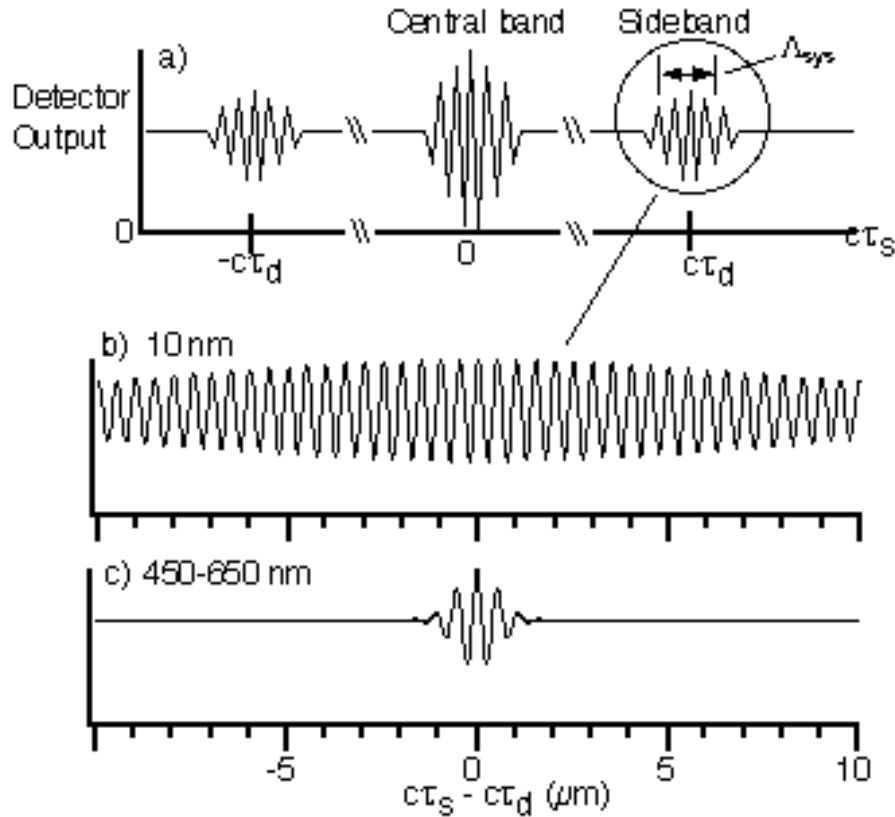


**Fig. 2.** White light velocimeter output versus source interferometer delay length ( $c\tau_s$ ), for a stationary target. Both source and detecting interferometers are the Michelson type. A moving target Doppler shifts apparent  $c\tau_s$  by  $(c\tau_s) = -(2v/c)(c\tau_s)$ . a) Schematic of global behavior: sidebands have the same shape and width as the central band, but lower amplitude. Their width, the system coherence length ( $\Lambda_{sys}$ ), is inversely proportional to the bandwidth of the system spectra. b) Calculated detail for 495-505 nm gaussian shaped system spectra. c) For 450 - 650 nm bandwidth.

In general, there is no restriction on the type of either interferometer. However, interpretation of the fringe shift is most straightforward when the detecting interferometer is of a Michelson type. In order for the velocimeter to work with illumination from an extended spatially incoherent source, both interferometers must satisfy the *superposition condition*: the images associated with each echo from the interferometer must superimpose. This way the ray paths of all echoes leaving the interferometer superimpose and the apparatus can be analyzed simply in the time domain. This can be accomplished by use of virtual or real imaging to create an apparent mirror which is superimposed on the mirror of the other arm. In our demonstration, the same optical system performs the functions of both the source and the detecting interferometers. This makes alignment much easier, because  $s_d$  automatically. However, in applications where the illumination is very much brighter than the light reflected from the target, the

source and detecting interferometers should be separate to isolate the glare of illuminating light from shared optics.

The Doppler effect scales the spectrum of the source interferometer by a factor  $(1+2v/c)$ . Since this spectrum's periodicity is controlled by  $c_s$ , this is equivalent to scaling the apparent value of  $c_s$  to  $c_s/(1+2v/c)$ . Hence, there is an apparent shift in  $c_s$  of

$$(c_s) = \frac{c_s}{1 + 2v/c} - c_s = -\frac{2v}{c} c_s. \quad (2)$$

Figure 2 shows the calculated fringes versus  $c_s$ , for the case of Michelson source and detecting interferometers and a stationary target. Fringe behavior versus velocity is obtained from these curves by shifting the initial value of  $c_s$  by the amount  $(c_s)$  given by (2).

The fringe visibility is defined  $(I_{\max}-I_{\min})/(I_{\max}+I_{\min})$ , where  $I_{\max}$  and  $I_{\min}$  are local maximum and minimum output intensities. As Fig. 2 shows, to obtain significant fringe visibility one needs  $c_s \approx c_d$ , within a distance we call the system coherence length  $l_{\text{sys}}$ . If  $\Delta$  is the system bandwidth, then the system coherence length is  $l_{\text{sys}} \sim 2/\Delta$ . Thus, inserting a narrow bandpass filter anywhere along the optical path can reduce and hence increase  $l_{\text{sys}}$ . For Michelson source and detecting interferometers, the fringe visibility does not exceed 50%. This is not a practical difficulty: because the two outputs of the detecting interferometer are of opposite phase, if they are both recorded they can be subtracted numerically to cancel the nonfringing signal portion. Also, using a Fabry-Perot source interferometer can increase fringe visibility arbitrarily at the expense of decreased absolute signal amplitude, depending on the Fabry-Perot mirror reflectivity  $R$ .

We demonstrate white light velocity interferometry by photographing the fringes from a 16 m/s moving target with incandescent light. Velocities of this order are more challenging to measure than velocities of order 1 km/s because of the smaller Doppler shifts. These are resolved by larger values of  $c$ , which in turn require larger diameter optics for a given angular field of view. Figure 3 describes our white light velocimeter having  $c_s \approx c_d = 4$  m and  $\Delta = 19$  m/s per fringe. By retro-reflecting the light from the target the functions of the source and detecting Michelson interferometers are accomplished by the same optics. This automatically insures that  $c_d \approx c_s$ . The interferometer mirrors are misaligned slightly to produce a ladder of fringes to make them more apparent.

An interferometer delay of 4 m is accomplished by the optics enclosed by the dashed box in Fig. 3. These create a virtual plane mirror, from a ray tracing aspect, but a delay of 4 m in the time-of-flight of a wave packet. The target was an electric fan with reflective tape on its blades. The beam intercepted the blade from 45 to 54 mm radius, at

an angle to the rotation plane of  $20.5^\circ$ . The frequency of rotation was determined stroboscopically to be 53.8 Hz. This yields a velocity component of  $15.7 \pm 3$  m/s parallel to the light. (The uncertainty is in the average fan radius struck by the beam.)

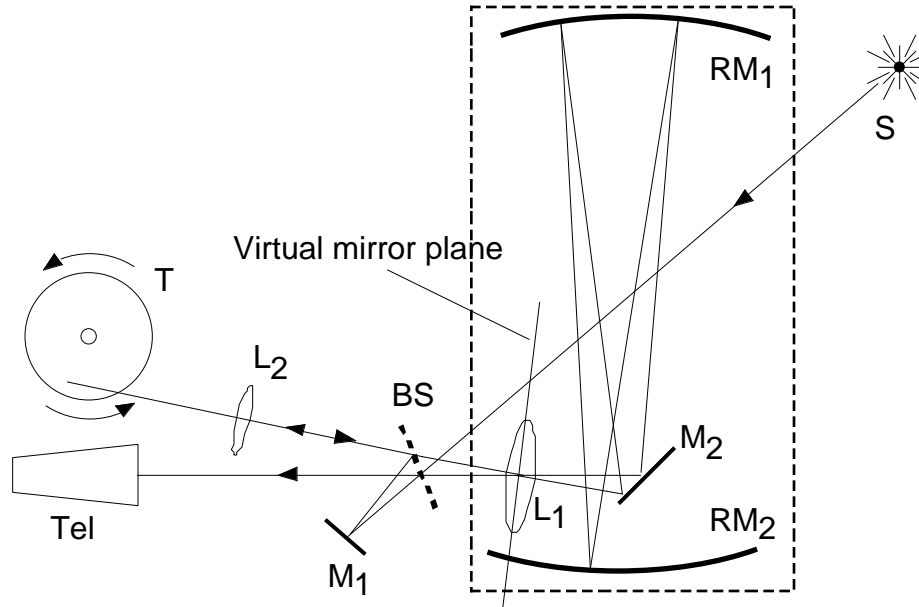


**Fig. 3.** White light velocimeter having 4 m delay and 19 m/s per fringe. This is a Michelson with a relay lens arm. S: incandescent lamp; T: target is fan with reflective tape on blades; Tel: telescope or camera; BS: 50% beamsplitter;  $M_1$ ,  $M_2$ : plane mirrors;  $RM_1$ ,  $RM_2$  mirrors having 1 m radius of curvature separated 1 m;  $L_1$ : 1 m focal length lens. Optics in dashed box act as virtual plane mirror at a position superimposed on reflective image of  $M_1$  about BS.  $L_2$ : lens images target to virtual mirror plane. Because light retro-reflects from target, the same optics performs source and detecting interferometer functions. The other interferometer output (not used here) travels toward the source and is accessible by inserting a beamsplitter between BS and S.

Figure 4 compares photographs of fringes from the stationary and moving target. The fringe pattern has visibly shifted toward the reference triangle due to target velocity. Observation through a 40 nm wide 500 nm bandpass filter shows the fringe shift to be  $0.85 \pm 0.07$ . For  $c = 4$  m and  $\lambda = 500$  nm,  $\lambda/c = 18.7$  m/s per fringe from Eq. (1). This yields an interferometrically measured velocity of  $15.9 \pm 1$  m/s. This agrees with the  $15.7 \pm 3$  m/s value measured stroboscopically.

The significance of this demonstration is two-fold. First, we observe fringes from an incoherent source with an interferometer delay greatly exceeding the  $\sim 1.5 \mu\text{m}$  coherence length of white light. Secondly, we demonstrate a fringe shift with target velocity, and this is a low velocity (by shock physics standards) measured remotely using easily obtained optics and an inexpensive light source.

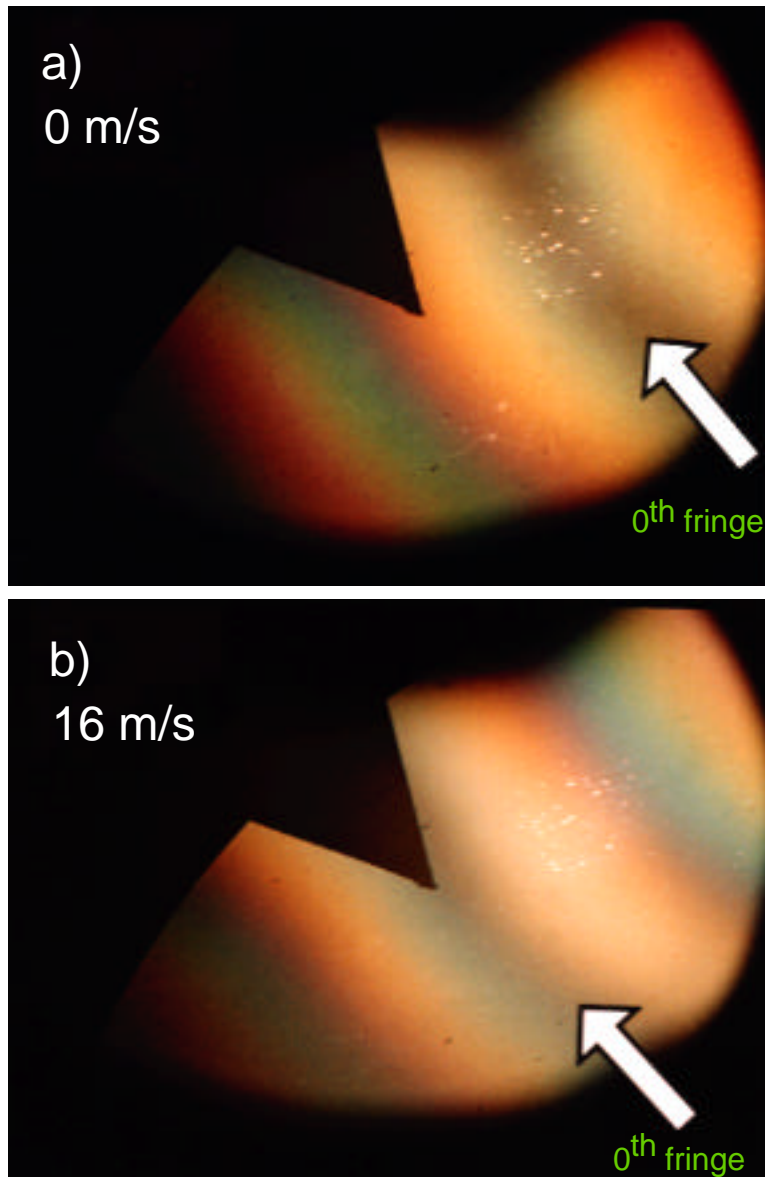


**Fig. 4.** White light fringes of target. a) Stationary target ; b) target moving at 15.7 m/s. Triangle silhouette at image plane ( $RM_1$ ) provides reference location. The dark central fringe (white arrows) can be distinguished by its colorless gray appearance and symmetrical placement relative to colored fringes, particularly the red fringes. From a) to b) the central fringe has shifted toward the triangle. When viewed in 500 nm light the shift is 0.85 fringe. The bright flecks are dust specks on  $RM_1$  illuminated by the source beam.

Because a conventional VISAR uses monochromatic illumination, a discontinuous velocity jump will cause an ambiguity in the fringe shift to an integer. This because fringes are periodic. However in the white light velocimeter, by recording fringe shifts for different colors separately, the velocity can be uniquely determined. One implementation of this is to disperse the velocimeter output by a grating and record the

spectrum versus time by a multi-channel detector or streak camera. The number of fringes across the streak record in the wavelength direction scales with the velocity, and therefore the velocity skip across the shock is determinate.

Our demonstration measured the velocity of a small area of the fan blade due to the limited angular field of view afforded by the optics we had on hand. We are constructing a new velocimeter with separate source and detecting interferometers, which will allow much brighter illumination with a wider field of view.

The white light velocimeter should lead to many new applications of velocimetry made practical by inexpensive or powerful incoherent sources. For example, a fluid velocity field could be measured over a large area on a microsecond or nanosecond time scale to high precision. This could aid in the study of turbulence. The ultimate spatial resolution would be superior to conventional fluid Doppler velocimetry<sup>18</sup> (where particles cross a standing fringe pattern formed by intersecting laser beams) because the speckle of white light is negligibly small, and because this fluid technique is limited to measurement at a single point. Interferometers implemented with single mode optical fiber having kilometer delays could measure mm/s velocities, although for a single target point. Such velocity sensitivity has already been demonstrated in a fiber optic Sagnac<sup>16</sup> interferometer design having a 200 m delay. In our design, the target is external to the interferometer, which allows practical velocimetry of remote targets in the field. The principle can be applied to other wave phenomenon such as microwaves and ultrasound.

**ACKNOWLEDGMENTS.** Work at Lawrence Livermore Laboratory was performed under auspices of US DoE contract No. W-7405-ENG-48.



## References

1. Atkinson, P. & Woodcock, J.P. Doppler Ultrasound and its Use in Clinical Measurement (Academic, New York, 1982).
2. Barker, L.M., & Hollenbach, R.E., J. Appl. Phys. 43, 4669-4675 (1972).
3. Barker, L.M., & Schuler, K.W., J. Appl. Phys. 45, 3692-3696 (1974).
4. Hemsing, W.F., Rev. Sci. Instrum. 50, 73-78 (1979).
5. Sweatt, W., Rev. Sci. Instrum. 63, 2945-2949 (1992).
6. Erskine, D.J., and Nellis, W.J., Nature 349, 317-319 (1991).
7. Erskine, D.J., and Nellis, W.J., J. Appl. Phys. 71, 4882-4886 (1992).
8. Erskine, D.J., and Nellis, J. Geophys. Res. 99, 15529-15537 (1994).
9. Taylor, G.I., Proc. Royal. Soc. Lndn A201, 192-196 (1950).
10. Richtmeyer, R.D., Comm. Pure Appl. Math 13, 297-319 (1960).
11. Hemsing, W.F., in *Shock Compression of Condensed Matter-1991*, edited by S.C. Schmidt et al., (North-Holland, Amsterdam, 1992), p. 767-770.
12. Delisle, C., & Cielo, P., Can. J. Phys., 53, 1047-1053 (1975).
13. Brooks, J., Wentworth, H., Youngquist, M., Kim, B.Y., Shaw, H., J. Lightwave Tech., LT-3, 1062-1071 (1985).
14. Gusmeroli, V., & Martinelli, M., Opt. Lett. 16, 1358-1359 (1991).
15. Ribeiro, A., Santos, J., Jackson, D., Rev. Sci. Instr. 63, 3586-3589 (1992).
16. Harvey, D., McBride, R., Barton, J., & Jones, J., Meas. Sci. Technol. 3, 1077-1083 (1992).
17. Geindre, J.; Audebert, P., Rousee, A.; Fallières, F., Gauthier, J.; Mysyrowicz, A.; Dos Santos, A.; Hamoniaux, G.; & Antonetti, A., Opt. Lett. 19, 1997-1999 (1994).
18. Lagranja, J.L.; García-Palacín, J.I.; and Aísa, L.A.; Opt. Engnrng. 33, 2449-2460 (1994).
19. Gidon, S and Behar, G., Appl. Opt. 25, 1429-1433 (1986).